Available online at www.sciencedirect.com
SCIENCE DIRECT®
International Journal of Thermal Sciences 44 (2005) 11–20
International Journal of Thermal Sciences
www.elsevier.com/locate/ijts

# Using undercooling to measure the freezing points of aqueous solutions

Vincent Ayel [a,*], Olivier Lottin [b], Elena Popa [c], Hassan Peerhossaini [a]

[a] *Laboratoire de thermocinétique, CNRS UMR 6607, École polytechnique de l'université de Nantes, BP 50609, 44306 Nantes, France*
[b] *Laboratoire d'énergétique et de mécanique théorique et appliquée, UMR 7563 CNRS-INPL, université Henri Poincaré, BP 160-2, avenue de la Forêt de Haye, 54504 Vandoeuvre-lès-Nancy, France*
[c] *"Politehnica" University of Bucharest, Faculty of Mechanical Engineering Splaiul Independentei 313, 77206 Bucharest, Romania*

Received 16 December 2003; received in revised form 23 April 2004; accepted 27 April 2004

Available online 20 July 2004

**Abstract**

In this paper, a new type of sensor for in-line measurements of antifreeze mass fraction in aqueous solutions is described. Its principles of operation are based on the exploitation of the temperature rise that accompanies the freezing of an undercooled solution. Measurements are performed on small volume samples, taken from a distribution loop. The device operates in batch and is reliable, compact and robust. Tests carried out with carefully calibrated water–antifreeze mixtures shows that its application fields are fully compatible with the antifreeze concentrations usually encountered in cold distribution circuits. This sensor can also be used for the experimental determination of the freezing point of various water–antifreeze mixtures, its accuracy being confirmed, with mono propylene glycol and mono ethylene glycol, by comparison of our results to those of the literature. However, tests carried out with ethanol showed that its performances are still to be improved with this antifreeze.


*Keywords:* Freezing; Undercooling; Supercooling; Antifreeze; Ice slurry; Crystallisation; Phase transition

## 1. Introduction

The work presented here is motivated by the development of secondary loops in refrigeration systems to reduce atmospheric leakage of polluting primary refrigerant. The secondary refrigerants are most often liquid blends of water and a cryoprotectant and are sometimes cooled below the freezing point and used as two-phase solid–liquid mixtures. This latter technique opens up the possibility of exploiting the latent heat of ice to increase the apparent heat capacity of the mixture, thus improving the overall efficiency of the system. The ice–liquid mixtures (or ice slurries) are mainly produced by heavy, large and expensive heat exchangers. However, considerable development work on two-phase liquid–solid secondary refrigerants is under way in many countries and one can reasonably expect them soon to become convincing alternatives to direct expansion systems.

The quantity of cryoprotectant introduced in the ice–slurry loop must be carefully controlled since it governs the relation between the temperature and the ice content in the solid–liquid mixture. Furthermore, measuring both the temperature and the antifreeze mass fraction in the liquid lets one check whether the solid and liquid phases are in thermodynamic equilibrium.

The aim of this study is to develop a small and simple sensor for determining the freezing points of aqueous solutions. This sensor must be reliable and small enough to allow in-line measurements in future installations that yield information on the quantity of cryoprotectant in the loop, or even on the thermodynamic equilibrium of the two-phase mixture. The proposed method is based on the analysis of the temperature evolution of a small sample of liquid during cooling: it detects and exploits the sudden temperature increase that occurs with the appearance of the first ice crystals. The principle of this method has been discussed in part elsewhere [1,2]; here we report on the first experimental device built for quick in-line measurements.

The governing equations are presented in Section 2 of this paper. The sensor prototypes are described in Sections 3

* Corresponding author.
*E-mail addresses:* vincent.ayel@polytech.univ-nantes.fr (V. Ayel), olivier.lottin@ensem.inpl-nancy.fr (O. Lottin), hassan.peerhossaini@polytech.univ-nantes.fr (H. Peerhossaini).

1290-0729/$ – see front matter 
doi:10.1016/j.ijthermalsci.2004.04.012

**Nomenclature**

| | | |
|---|---|---|
| $c_p$ | heat capacity | $J{\cdot}kg^{-1}{\cdot}K^{-1}$ |
| $h$ | enthalpy | $J{\cdot}kg^{-1}$ |
| $L_f$ | latent heat of phase change | $J{\cdot}kg^{-1}$ |
| $m$ | mass | kg |
| $Q$ | heat loss | J |
| $t$ | time | s |
| $T$ | temperature | °C |
| $x_a$ | antifreeze mass fraction | $kg{\cdot}kg^{-1}$ |
| $x_s$ | ice mass fraction | $kg{\cdot}kg^{-1}$ |

*Greek symbols*

| | | |
|---|---|---|
| $\phi$ | heat flux | W |
| $\varepsilon$ | absolute error | |

*Subscripts*

| | |
|---|---|
| $c$ | beginning of crystallisation |
| $eq$ | thermodynamic equilibrium |
| $i$ | initial |
| $l$ | liquid phase |
| $mc$ | maximum temperature of crystallisation |
| $s$ | solid phase |
| $w$ | water |

and 4, and Section 5 details the results of a complete error calculation, providing information on the sensor's reliability and accuracy. Results of tests carried out under real operating conditions are given in Section 6.

## 2. Governing equations

### 2.1. Enthalpy of the solution

Below the freezing point, the mass enthalpy of an ice–liquid solution is the sum of the mass enthalpies of ice and of the liquid mixture, both at the same temperature:

$$h(T) = x_s h_s(T) + (1 - x_s) h_l(T, x_{a,l}) \tag{1}$$

The ice mass fraction is a function of the antifreeze mass fraction in the whole solid and liquid mixture $x_{a,i}$ and in the residual liquid $x_{a,l}$. $x_{a,i}$ is also the initial mass fraction of the diluted compound in the liquid mixture before freezing and is given by the freezing diagram as a function of temperature:

$$x_s(T) = 1 - \frac{x_{a,i}}{x_{a,l}(T)} \quad \text{or} \quad x_{a,l}(T) = \frac{x_{a,i}}{1 - x_s(T)} \tag{2}$$

The mass enthalpies of both pure water and antifreeze in the reference state, i.e., at 0 °C and in the liquid phase, are 0 J. Thus, the mass enthalpy of ice can be calculated as:

$$h_s(T) = \int_0^T c_{p,s}(T)\,\mathrm{d}T - L_f \tag{3}$$

The mass heat capacity of ice is well known. We use the linear equation of Bel and Lallemand [3]:

$$c_{p,s}(T) = 2.1162 + 0.0078T \tag{4}$$

The enthalpy of the liquid phase $h_l$ depends on the antifreeze concentration and on the temperature:

$$h_l(T, x_{a,l}) = \left[\int_0^T c_{p,l}(T, x_{a,l})\,\mathrm{d}T\right]_{x_{a,l}} + \Delta_{mix} h_l(0\,°\mathrm{C}, x_{a,l}) \tag{5}$$

$\Delta_{mix} h_l(0\,°\mathrm{C}, x_{a,l})$ is the heat of mixing of the two substances at 0 °C, which values are available in the literature (Melinder [4]). This enthalpy model is valid provided the temperature of the sample is uniform and the solid and liquid phases are in thermodynamic equilibrium. The contact energy between ice crystals and the solution is neglected.

In order to apply this model to each kind of aqueous mixture, it is necessary to know the heat capacity of the liquid phase and, as precisely as possible, the freezing curve over the complete temperature and concentration ranges. The mass heat capacities of the most commonly used water–antifreeze mixtures have been determined and published by Melinder [5,6]. The reliability of these data when used to calculate the thermodynamic properties of commercial products, which include some additives, can be discussed: even small amounts of additives can significantly modify the shape of the freezing curve.

### 2.2. Undercooling

Knowing the antifreeze mass fraction $x_{a,i}$ in a liquid water–antifreeze mixture, makes it possible to determine, by means of the freezing curve, its temperature of thermodynamic equilibrium with ice $T_{eq}(x_{a,i})$. However, most liquids, and in particular water–antifreeze mixtures of interest in this study, crystallize only if they pass through the so-called undercooled state (Papon et al. [7]), which corresponds to the persistence of the liquid state, without any solid crystal, at temperatures below the transition temperature $T_{eq}$. At these temperatures, the most thermodynamically stable state would be the pure ice with a liquid solution at $x_{a,l}$ and thus the undercooled solution at $x_{a,i}$ is described as "metastable".

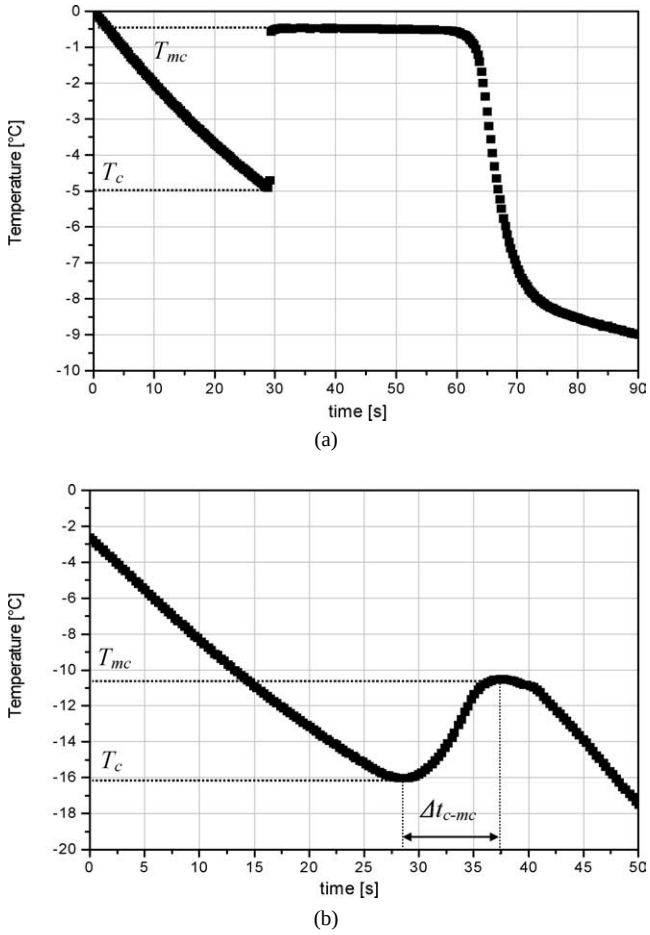


Fig. 1. Temperature evolution during cooling of a small-volume water–antifreeze sample: (a) $x_{a,i} = 0.02$, (b) $x_{a,i} = 0.25$.

Crystallisation occurs at an initial temperature of crystallisation $T_c$ below $T_{eq}$: if the difference between $T_c$ and $T_{eq}$ is sufficient and if the kinetics of crystallisation is fast enough, the ice mass fraction increases homogeneously and quickly throughout the entire sample. However, due to limiting phenomena such as thermal diffusion or slow crystalline growth, the transition between the metastable undercooled state and stable thermodynamic equilibrium is, in most cases, not immediate. Statistical studies have shown that the temperature of the beginning of crystallisation $T_c$ is randomly distributed but is influenced by the volume of the sample, the presence of foreign bodies, the thermal history and the cooling rate (Okawa et al. [8,9]).

Crystallisation of the undercooled liquid mixture results in a temperature increase due to the release of the latent heat of ice (Fig. 1). If the mixture is cooled down continuously, the temperature then reaches a maximum before decreasing again. This maximum value and its time of occurrence depend on many factors such as the volume, the cooling rate, the antifreeze mass fraction, the temperature of onset of crystallisation and the position (since the ice grows progressively in the sample from the location of the appearance of the first crystal, even if the temperature is homogeneous). It must be noted that due to the increase in the antifreeze mass fraction in the residual liquid (linked to the appearance of ice) and to the energy exchanged, the maximum temperature of crystallisation of binary mixtures is necessarily lower than the solid–liquid equilibrium temperature of the initial mixture $T_{eq}(x_{a,i})$.

### 2.3. Use of the temperature increase due to crystallisation during the cooling of a small-volume sample

Evolution of the mixture between $T_c$ and $T_{mc}$ can be regarded as an isenthalpic phenomenon if it happens over a sufficiently short time period (Fig. 1(a)). However, when the concentration of antifreeze is high, it can be useful to take into account the quantity of heat removed from the sample during $\Delta t_{c\text{–}mc}$ (Fig. 1(b)). The difference in behaviour between Fig. 1(a) and (b) is due to the kinetics of crystallisation. The transition from liquid to solid state is not instantaneous and the material evolves during the transformation. Crystal growth is fast when the antifreeze mass fraction is low: once the germs exceed a critical size, they can continue growing while moving easily in the medium and interacting with the others. When the antifreeze mass fraction is higher, the viscosity of the medium becomes more significant and limits the displacement of the molecules. The presence of a substance that does not solidify limits the interactions between ice nucleus and crystal growth takes more time (Fig. 1(b)).

Exploitation of single-point temperature measurements and use of the enthalpy model described in Section 2.1 are possible only if the sample temperature can be considered homogeneous in space. Such a condition can be reached by stirring the mixture continuously, but at the expense of compactness and cooling rate [1,2]. To overcome this difficulty, vessels of very small size are used (typically 0.1 $cm^3$); in the following, *the sample temperature is always assumed to be homogeneous*. Furthermore, the sample rate of cooling is assumed sufficiently low so that *the liquid and solid phases can be considered in thermodynamic equilibrium*. Starting from this, the return to equilibrium that follows the beginning of crystallisation ends when the whole sample is again in a stable equilibrium state: once the maximum temperature of crystallisation ($T_{mc}$, Fig. 1) is reached, the antifreeze mass fraction in the residual liquid is related to the temperature by the freezing curve—i.e., $\forall T \leqslant T_{mc}$, $\forall t \geqslant t_{mc}$, $T = T_{eq}(x_{a,l})$—and to the initial mass fraction by Eq. (2). However, Eq. (2) is useless without knowledge of the ice mass fraction, which we lack: consequently, neither $T_{mc}$ nor the temperatures recorded after crystallisation began provide any direct information about the freezing curve of the water–antifreeze mixture. In fact, $T_{mc}$ is a reliable estimate of $T_{eq}(x_{a,i})$ only if the antifreeze mass fraction is low, as illustrated by Fig. 2.

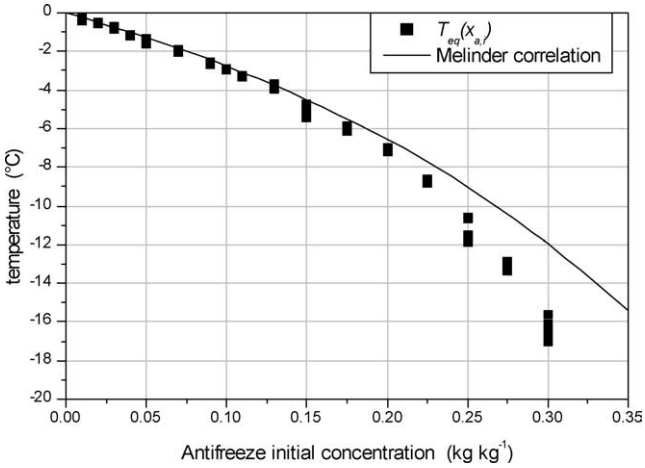


Fig. 2. Estimation of $T_{eq}(x_{a,i})$ from the direct measurement of $T_{mc}$ (for MPG): this method is not valid for antifreeze concentration above 0.1.

Considering the energy removed from the sample between $T_c$ and $T_{mc}$ as equal to $Q$ (in Joule) and applying an enthalpy balance leads to

$$mh_l(T_c, x_{a,i}) = (m - m_s)h_l(T_{mc}, x_{a,mc}) + m_s h_s(T_{mc}) + Q \tag{6}$$

The ice mass fraction and the mass fraction of antifreeze in the residual liquid at the maximum crystallisation temperature are given by the following relations, which are easily solved in a few iterations:

$$\begin{aligned} x_s(T_{mc}) &= \frac{m_s}{m} = \frac{h_l(T_c, x_{a,i}) - h_l(T_{mc}, x_{a,mc}) - Q/m}{h_s(T_{mc}) - h_l(T_{mc}, x_{a,mc})} \\ x_{a,mc} &= x_{a,i}\frac{h_s(T_{mc}) - h_l(T_{mc}, x_{a,i}/(1 - x_s))}{h_s(T_{mc}) - h_l(T_c, x_{a,i}) + Q/m} \end{aligned} \tag{7}$$

The last form of Eq. (7) is used to determine the freezing curve of water–antifreeze mixtures by using experimental values of $T_{mc}$ and the values of $x_{a,mc}$ which result from them. It is valid only if the liquid and the solid phases are assumed to be in thermodynamic equilibrium. It is also possible to evaluate by means of Eq. (7) the initial quantity of antifreeze $x_{a,i}$ in the sample, from the knowledge of $T_c$, $T_{mc}$ (both measured): in this case, assuming thermodynamic equilibrium, $x_{a,mc}(T_{mc})$ is given by the freezing curve and $x_{a,i}$ is deduced by inverting (numerically) the last form of Eq. (7).

Strictly speaking, the heat removal between $t_c$ and $t_{mc}$ is:

$$Q = \int_{\Delta t_{c-mc}} \varphi(T, t)\,\mathrm{d}t \tag{8}$$

Knowing the mass of the sample $m$, $\varphi(T, t)$ is estimated from the temperature evolution throughout cooling until undercooling ceases. Thanks to a least-square fitting, correlations giving values of $\partial T/\partial t$ as a function of $T$ are established numerically at each recording. For the sake of simplicity, $\varphi(T)$ is evaluated at $(T_c + T_{mc})/2$ and the estimated value of the heat removal becomes

$$[Q]_{ESTIMATED} = \varphi\left(\frac{T_c + T_{mc}}{2}\right)\Delta t_{c-mc} \tag{9}$$

with

$$\begin{aligned} &\varphi\left(\frac{T_c + T_{mc}}{2}\right) \\ &\quad = m \cdot c_p\left(\frac{T_c + T_{mc}}{2}, x_{a,i}\right)\frac{\partial T}{\partial t}\left(\frac{T_c + T_{mc}}{2}\right) \end{aligned} \tag{10}$$

It must be kept in mind that the evaluation method described above yields only a rough estimate of the heat removal between $t_c$ and $t_{mc}$. Its main advantage is that it can be implemented with no further information than the temperature recording and the sample mass (which is easily known from the vessel volume and the knowledge of $x_{a,i}$). However, this method underestimates the heat flux since the temperature difference between the sample and the copper walls increases when undercooling ceases.

## 3. Experimental apparatus

Experiments were carried out with two sets of apparatus:

- A calibration bench (Fig. 3), used to test the validity of the method by comparing the data on solid–liquid thermodynamic equilibrium ($x_{a,mc}$, $T_{mc}$) to the correlations of Melinder [5,6].
- A prototype in-line sensor (Figs. 4, 5), used to validate the operation of the system under actual industrial working conditions by comparing measurements of the antifreeze mass fraction ($x_{a,i}$) to carefully calibrated values.

### 3.1. Calibration bench

The calibration bench, used to determine the freezing curve of water–antifreeze mixtures, consists simply of a hollow copper cube in which the sample is placed. A plastic plug closes the cavity (a cylinder whose diameter and height are both 5 mm) and the sample temperature is measured by a micro-thermocouple inserted through the plug. In order to minimize the thermal inertia of the thermocouple, the diameter of the wires must be between 50 and 80 μm. The copper vessel is refrigerated by means of four thermoelectric Peltier modules that eject heat towards two water-cooled metal holders. The total surface of the four Peltier modules is 64 cm$^2$. The electrical power is about 100 W which, depending on the temperature, provides a cooling power lower than 1 W in the sample. The cooling rate of the sample is no more than $-0.5$ °C per second at 0 °C.

A data recording and processing system was used to analyse the temperature evolution as a function of time. Experiments and calibrations were done on samples of

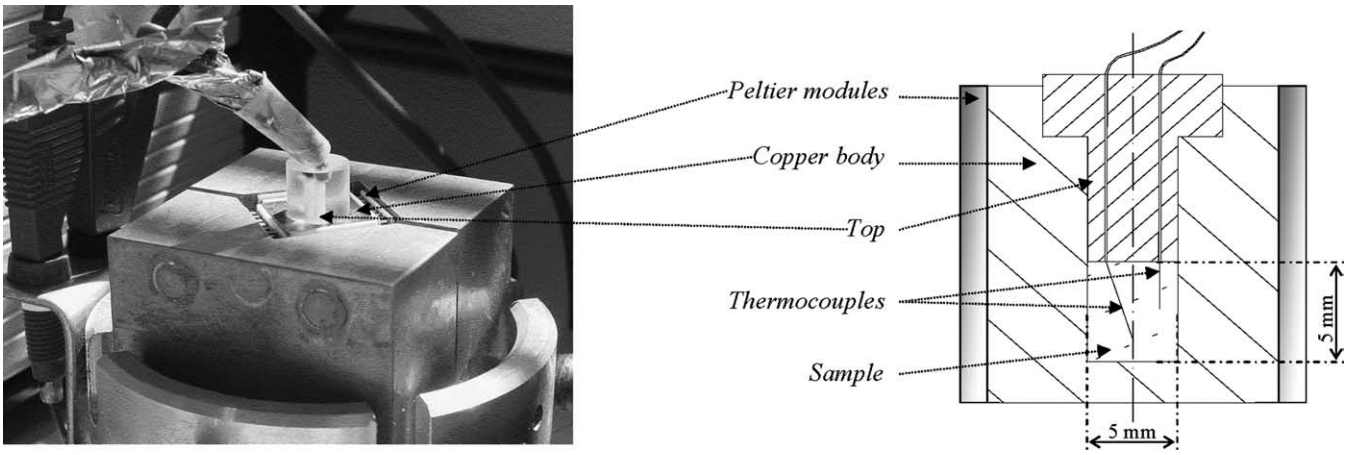


Fig. 3. Calibration bench.

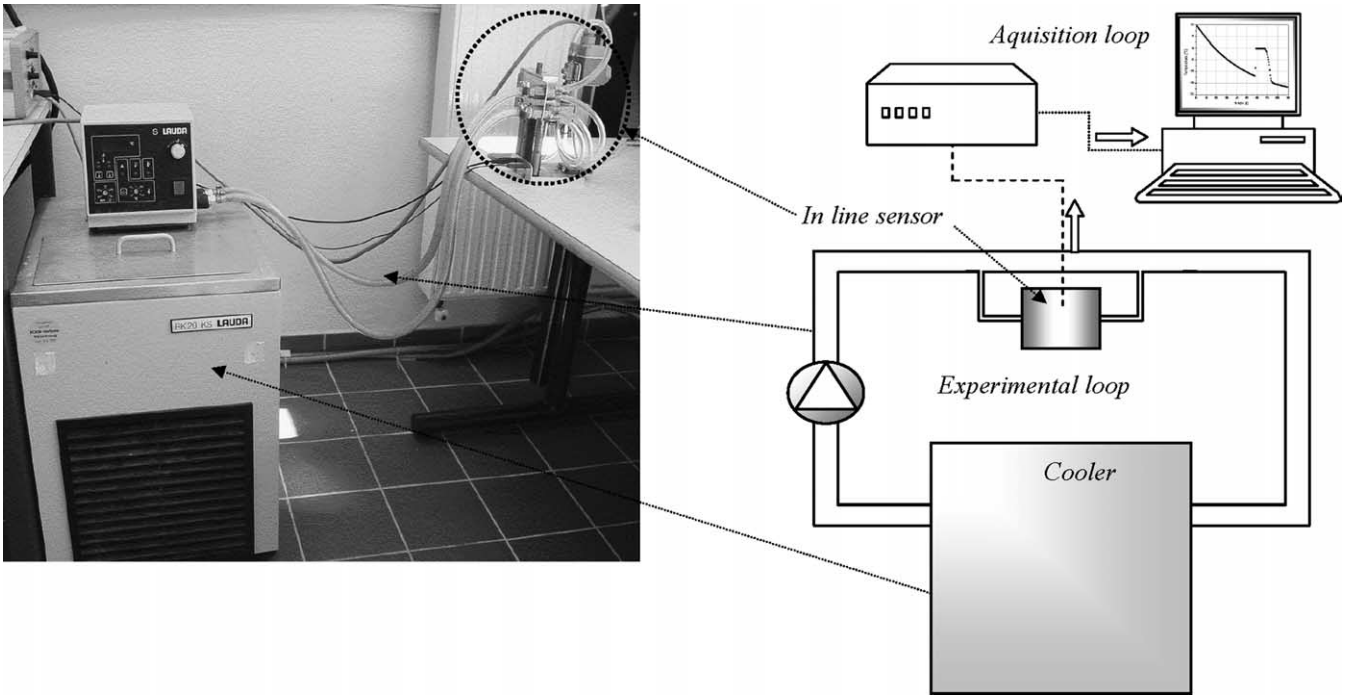


Fig. 4. In-line sensor, global experimental loop.

monopropylene glycol (MPG) of concentrations ranging between 1 and 30% in weight, and on samples of ethanol and monoethylene glycol (MEG) of concentrations ranging between 5 and 30% in weight.

### *3.2. In-line sensor*

The in-line sensor is used to determine the amount of antifreeze in a liquid sample when the freezing curve is known (Figs. 4 and 5). It works on the same principles as the calibration bench (sample contained in a copper vessel surrounded by four Peltier modules cooling the unit), except that the apparatus is connected to a loop in which a secondary refrigerant of known concentration circulates in the liquid state. For test purposes, the antifreeze mass fraction measured by the apparatus is directly compared to the quantities introduced in the loop. The thermoelectric Peltier modules are cooled, through the holders, by the secondary refrigerant, which improves their efficiency. An electromagnetic valve controls samplings. The results of tests carried out for antifreeze mass fractions of 5, 10, 15, 20, 25 and 30% are presented in Section 6.

## 4. Experimental results with calibration bench

The results of the calibration tests are plotted in Fig. 6(a) for the three different antifreezes. The dotted and solid curves represent the correlations of Melinder [5,6]. The experimental data are in good accordance with the general

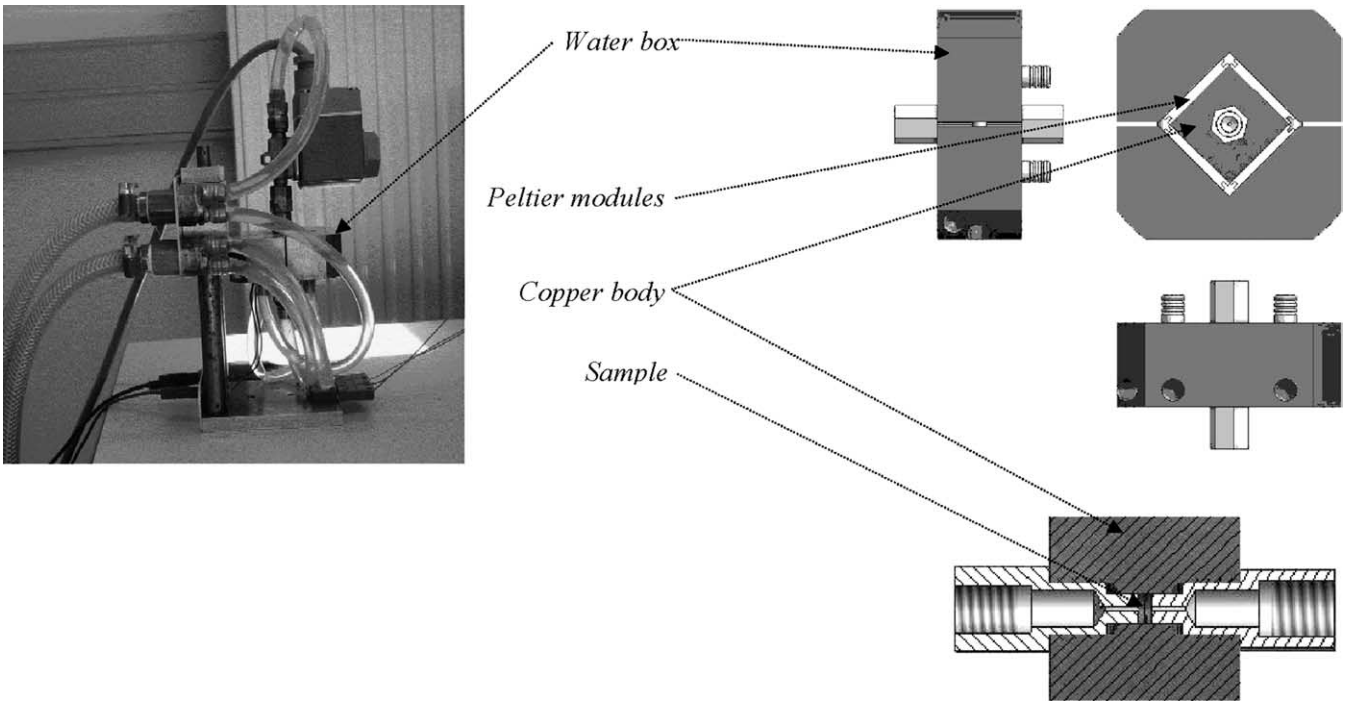


Fig. 5. In-line sensor, detailed parts of the sensor.

trend of the equilibrium curves from the literature, but they deviate for higher concentrations, particularly with ethanol, the shape of which experimental curve differs strongly from Melinder's data. The process of crystal growth between $t_c$ and $t_{mc}$ is more complex and is probably slowed down by surface tension effects. Taking into account the heat removal during solidification $Q$ seems to improve the results (Fig. 6(b)), but on the other hand, the points above the curve are shifted for the lowest concentrations (less than 20%). The difference between data from the literature and our experimental results can be explained by the overall inaccuracy of the measuring method, especially at the highest antifreeze concentrations, or by a variation in sample composition. Indeed, except with ethanol that was pure, the calibration tests were carried out with commercial antifreezes that can include additives of often unknown quantity. In order to investigate these two hypotheses, an error analysis is presented below (Section 5) and the experimental correlations are used when processing the data measured by the in-line sensor.

## 5. Error analysis

The following analysis starts from the tests carried out on MPG on the calibration bench and is applied to the determination of $x_{a,mc}$, $x_{a,i}$ being known. The same procedures could be applied to the other antifreezes (ethanol or MEG) and to the determination of $x_{a,i}$ when the correlation of $T_{mc}$ and $x_{a,mc}$ is known. Possible sources of inaccuracy are linked to:

- the measurement of the system variables: $x_{a,i}$, $T_c$ and $T_{mc}$;
- the evaluation of the heat capacity of the liquid mixture: $c_p$;
- the hypotheses on which the calculations are based: $\Delta t_{c-mc} = 0$.

The following error analysis consists in evaluating the error on $x_{a,mc}$ starting from the uncertainty of measurements on the preceding parameters.

### 5.1. Influence of the antifreeze initial concentration $x_{a,i}$

The uncertainty of $x_{a,i}$ measurements is evaluated as follows:

$$x_{a,i} = \frac{m_{a,i}}{m_{a,i} + m_w} \tag{11}$$

$$\Delta x_{a,i} = \frac{m_w \varepsilon(m_{a,i}) + m_{a,i}\varepsilon(m_w)}{m_{a,i}(m_{a,i} + m_w)} \tag{12}$$

where $\varepsilon(m_w)$ and $\varepsilon(m_{a,i})$ (respectively 0.025 and 0.01 g) are the resolution of the water and antifreeze weighing devices, respectively. Using the results of Eqs. (11) and (12) to the error calculation at each antifreeze concentration shows that the error related to $x_{a,mc}$ never exceeds 1.5% and becomes negligible for $x_{a,i}$ over 0.15.

### 5.2. Influence of the error in the temperature measurements ($T_c$ and $T_{mc}$)

Starting from recordings, with the same apparatus, of the crystallisation temperature of pure water, and looking

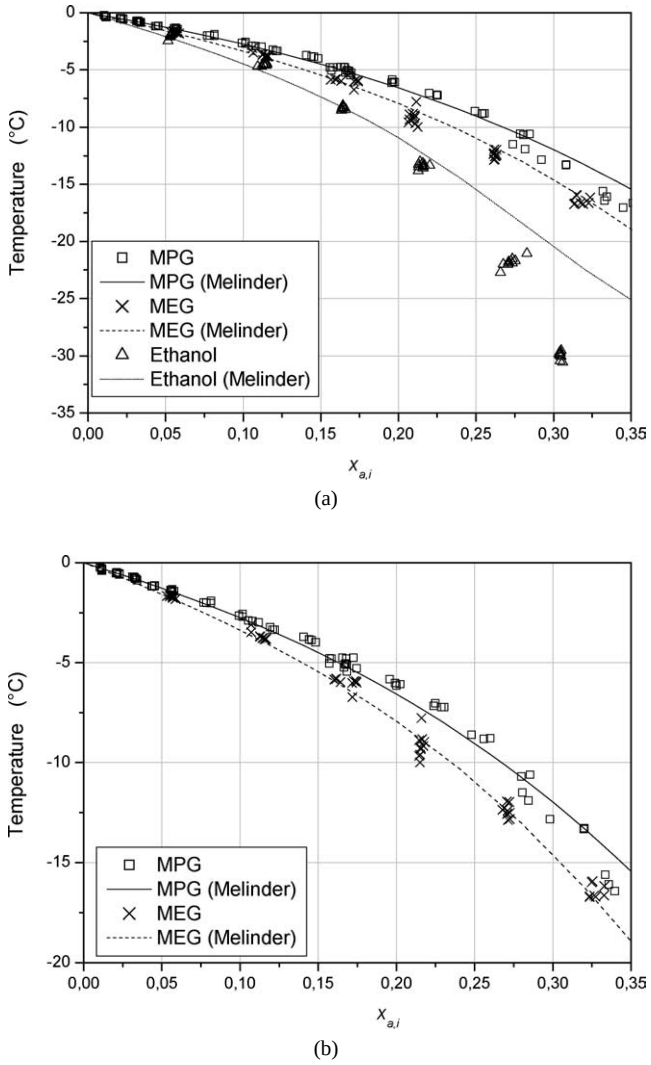


Fig. 6. Experimentally determined solidification curves of water–antifreeze mixtures: (a) For MPG, ethanol and MEG, without taking the heat loss $Q$ into account; (b) For MPG and MEG, taking the heat loss $Q$ into account. 123, 60 and 60 measurements were recorded for MPG, MEG and ethanol, respectively.

at the dispersion of the data around 0 °C, the uncertainty linked to the temperature measurement is estimated equal to $\Delta T = 0.05\,^{\circ}\mathrm{C}$. It is to be noted that these inaccuracies are due on the one hand to the data-acquisition system and on the other hand to local temperature variations in the sample during the freezing of water; the hypothesis of thermodynamic equilibrium is only an approximation of the real phenomena.

It is possible to obtain a first estimation of the error on $x_{a,mc}$ linked to the uncertainty of the temperature measurements by rewriting Eq. (7) as follows:

$$x_{a,mc} = F(h_{s,T_{mc}}, h_{l,T_{mc}}, h_{l,T_c}) = x_{a,i}\frac{h_{s,T_{mc}} - h_{l,T_{mc}}}{h_{s,T_{mc}} - h_{l,T_c} + Q/m} \tag{13}$$

Then, a simple error calculation leads to:

$$\frac{\Delta x_{a,mc}}{x_{a,mc}} \cong \Delta h_{s,T_{mc}}\frac{h_{l,T_c} - Q/m - h_{l,T_{mc}}}{(h_{l,T_c} - Q/m - h_{s,T_{mc}})(h_{l,T_{mc}} - h_{s,T_{mc}})} + \frac{\Delta h_{l,T_{mc}}}{h_{l,T_{mc}} - h_{s,T_{mc}}} + \frac{\Delta h_{l,T_c}}{h_{l,T_c} - Q/m - h_{s,T_{mc}}} \tag{14}$$

And, by assuming negligible $Q/m$ and the differences between liquid enthalpies $h_{l,T_{mc}}$ and $h_{l,T_c}$, Eq. (14) simplifies as:

$$\frac{\Delta x_{a,mc}}{x_{a,mc}} \cong \frac{\Delta h_{l,T_{mc}}}{h_{l,T_{mc}} - h_{s,T_{mc}}} + \frac{\Delta h_{l,T_c}}{h_{l,T_c} - Q/m - h_{s,T_{mc}}} \cong \frac{2c_{p,l}\Delta T}{L_f} \tag{15}$$

Eq. (15) is only a approximation that gives a relative error on $x_{a,mc}$ ($\approx 0.12\%$ with $\Delta T = 0.05$ K) of the same order of magnitude as the result of an exact error calculation ($\approx 0.2\%$ in Fig. 8(b)). Eq. (15) shows that the error does not depend much on the antifreeze mass fraction $x_{a,i}$ but rather on the ratio between the heat capacity of the liquid and the latent heat of phase change, which can be considered as constant. Indeed, the exact error calculation (Fig. 8(b)) shows that the influence of an error of 0.05 K in the temperature measurements ($T_c$ and $T_{mc}$) does not vary significantly, neither with $x_{a,i}$ (ranging from 0.05 kg·kg$^{-1}$ to 0.3 kg·kg$^{-1}$), nor with $T_{mc} - T_c$ (ranging from 1 to 10 °C).

### 5.3. Influence of the specific heat $c_p$

The values of $c_p$ used in calculating $x_{a,mc}$ and $x_s$ come from the work of Melinder [5,6]. The error induced in $x_{a,mc}$ is calculated starting from the deviation in $c_p$ indicated by Melinder (i.e., 0.166%). However, other sources of error are:

- The exact composition of the antifreeze; the presence of additives in the mixture may change the value of its heat capacity.
- Incomplete knowledge of the heat capacity of the water–antifreeze mixture at temperatures below the freezing temperature (in the undercooled state).

In order to evaluate the importance of these two sources of error, we multiplied by 10 the deviation of $c_p$ indicated in the literature. Even in this case, the relative error on $x_{a,mc}$ does not exceed 0.5‰. This result shows that the influence of the $c_p$ deviation, even due to the presence of additives, is certainly low compared to the other sources of uncertainty.

### 5.4. Influence of the heat flow Q during crystallisation

Fig. 7 shows that the time $\Delta t_{c\text{–}mc}$ between $T_c$ and $T_{mc}$ increases with $x_{a,i}$ and reaches values for which the heat removal $Q$ cannot be neglected in the enthalpy balance (Eq. (6)). Fig. 8(a) shows the relative magnitude of the

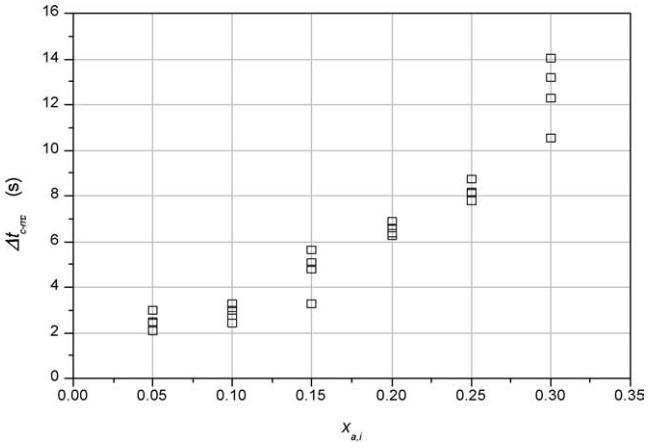


Fig. 7. Evolution of the time $\Delta t_{c-mc}$ between $T_c$ and $T_{mc}$ as a function of $x_{a,i}$.

Table 1
Comparison of the results from the calibration device and a correlation resulting from pre-tests carried out on the same bench

| Antifreeze | Deviation below 5% | Deviation below 10% | Deviation % below 15% |
|---|---|---|---|
| MPG | 96% | 100% | – |
| Ethanol | 74% | 88% | 96% |
| MEG | 86% | 100% | – |

correction induced by considering the heat losses. It is however, difficult to evaluate properly the accuracy of the determination of $Q$. In fact, due to the simplified method of evaluation used in Section 2.3, it might well be no better than 50%. Consequently, it can be concluded that the relative error in $x_{a,mc}$ due to the inaccuracy in the heat removal is about 4.5% in the worst case.

### 5.5. Global error analysis

Fig. 8(b) displays, as a function of $x_{a,i}$, the estimate of the global uncertainty of the measurement method, starting from the cumulative error resulting from the parameters previously cited. For the lowest antifreeze concentrations, the most significant source of error is the evaluation of the initial antifreeze concentration $x_{a,i}$. At higher antifreeze mass fraction, the error in the measurement of $T_{mc}$ and $T_c$ dominates. In all cases, the cumulative error due to $x_{a,i}$, $c_p$, $T_{mc}$ and $T_c$ is always below 0.3%. By comparison, the omission of the heat flux lost by the sample between $T_c$ and $T_{mc}$ (Fig. 8(a)) would imply relative variations in the results that would reach 4.5% when the antifreeze mass fraction is equal to 30%. The evaluation of $Q$ is in fact the most significant source of error. The use of heat flux sensors could improve the accuracy, but at the expense of the simplicity and reliability of the in-line sensor.

It must be noted that the error analysis presented above does not explain some of the variations between our results and those of the literature, in particular for ethanol (Fig. 6). Most probably, the assumption of temperature homogeneity

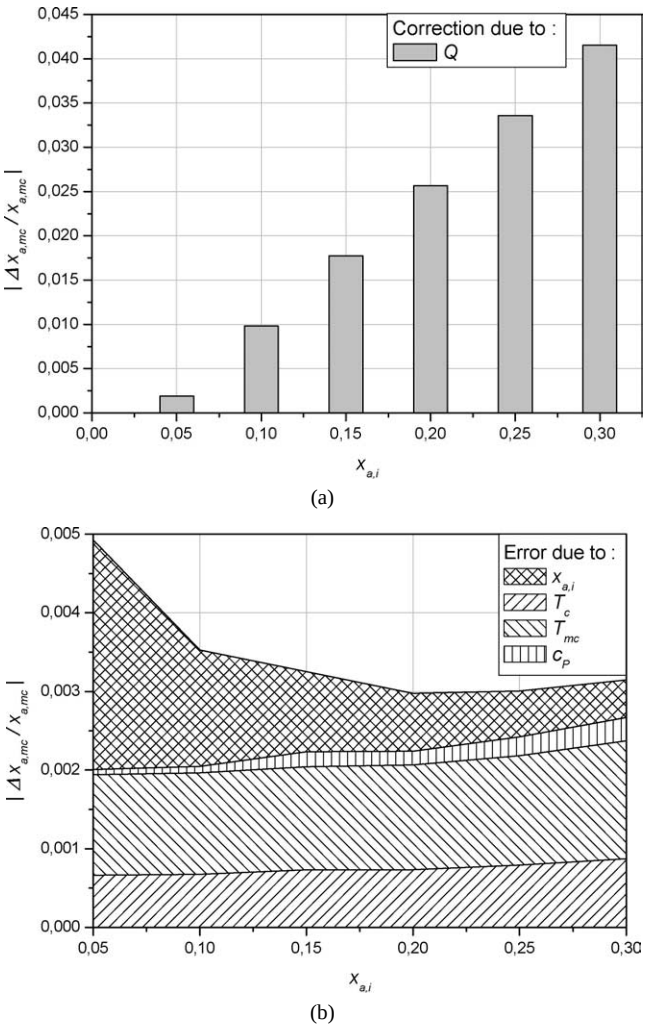


Fig. 8. Errors relating to $x_{a,mc}$ as a function of $x_{a,i}$: (a) Correction taking $Q$, into account; (b) Cumulative relative errors due to $x_{a,i}$, $T_c$, $T_{mc}$ and $c_p$.

in the sample is not valid in some cases. A detailed model of the crystallisation of undercooled water–antifreeze mixtures in small-volume vessels would provide useful information for improving the method. Comparison of $x_{a,mc}$ values measured with the calibration device and those given by the correlation resulting from pre-tests using the same bench shows that the results are reproducible (Table 1).

## 6. Experimental results for in-line measurements

The in-line sensor is designed to measure the mass fraction of antifreeze $x_{a,i}$ in liquid mixtures flowing in pipes. For test purposes, the in-line sensor is connected to a temperature-controlled loop containing cooled water–antifreeze blends of carefully calibrated concentration.

The freezing curves used for the determination of $x_{a,i}$ are those of Melinder [5,6] or ours, obtained from preliminary tests carried out with the calibration device (Section 5). Fig. 9(a), (b) present a comparison of results obtained with MPG in the best and worst conditions. On the one hand

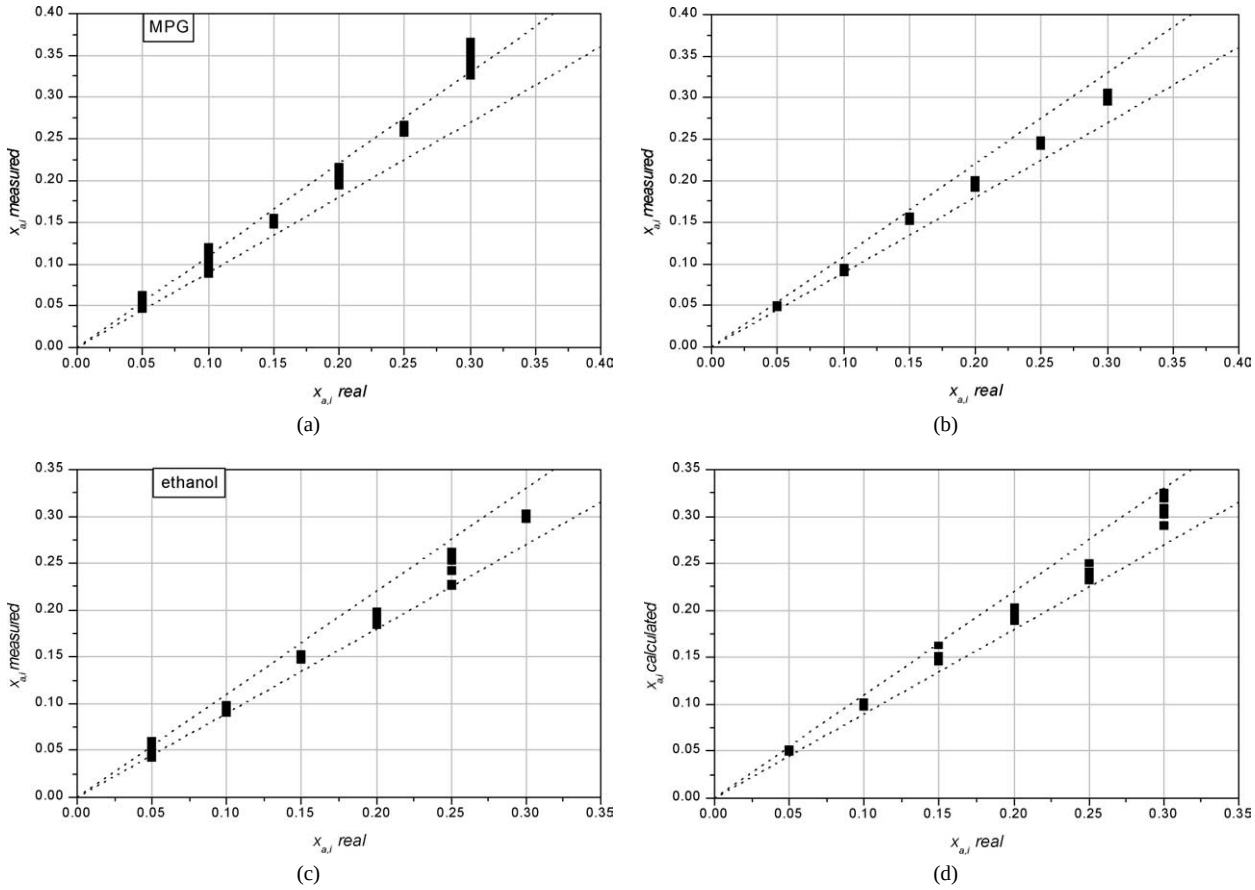


Fig. 9. Comparison of the values of $x_{a,i}$ calculated with the in-line sensor: (a) For MPG, $Q = 0$, Melinder correlation, with four cooling rates; (b) For MPG, $Q \neq 0$, calibrated correlation, only the highest cooling rate; (c) For ethanol, $Q \neq 0$, calibrated correlation, (d) For MEG, $Q \neq 0$, calibrated correlation. The domain within the dotted lines corresponds to relative variations of less than 10%. 183, 60 and 60 measurements were recorded for MPG, MEG and ethanol, respectively.

Table 2
Statistical analysis of the in-line sensor accuracy

| Antifreeze | Error below 5% | Error below 10% | Error below 15% |
|---|---|---|---|
| MPG (with Melinder's freezing curve) | 74% | 92% | 100% |
| MPG (with our freezing curve) | 83% | 100% | – |
| Ethanol | 64% | 94% | 97% |
| MEG | 83% | 100% | – |

Table 3
Mean relative error in $x_{a,i}$ measurements for all antifreeze concentrations and for the three antifreezes

| Antifreeze | $x_{a,i}$ | | | | | |
|---|---|---|---|---|---|---|
| | 0.05 | 0.10 | 0.15 | 0.20 | 0.25 | 0.30 |
| MPG | 1.9% | 5.7% | 2.7% | 2.2% | 1.9% | 0.9% |
| Ethanol | 9% | 6.9% | 1.1% | 3.9% | 5.7% | 0.5% |
| MEG | 2.2% | 1.1% | 1.9% | 3.6% | 4.8% | 3.2% |

(Fig. 9(a)), all the calculations are based on the freezing curves of the literature [5,6] without taking into account the heat removal $Q$ at various cooling rates. On the other hand (Fig. 9(b)), measurements are carried out with the highest cooling rate, the freezing curve resulting from calibration tests is used, and the heat removal $Q$ is taken into account. Fig. 9(c), (d) present results corresponding to the best configuration (taking into account the heat removal, with our calibrated curve, and at the maximum cooling rate) for ethanol and MEG, respectively. The dispersion of the results can be significantly decreased if the cooling rate is the same in all tests, including the calibration ones. Similarly, it is better to use a freezing curve determined by means of the calibration device, even if this curve deviates from the data of the literature at the highest antifreeze mass fractions. Indeed, this experimental freezing curve is modified by the crystallisation kinetics, but crystallisation occurs in the same way in the calibration device and in the in-line sensor. Tables 2 and 3 present a statistical analysis of the sensor accuracy; the error is more significant with ethanol for the lower concentrations, reaching an average of 9% ($x_{a,i} = 0.05$). For MPG, the error, averaged for each antifreeze mass fraction, does not exceed 6% ($x_{a,i} = 0.10$), whereas for MEG, this mean error does not exceed 5% ($x_{a,i} = 0.25$). The fact that MEG and MPG belong to the same group

of chemicals may explain their similar behavior in terms of sensor performances. Table 3 shows that there is no clear dependence of the accuracy on the antifreeze mass fraction.

## 7. Conclusions

The results presented here show the promise of measuring the freezing temperature of an aqueous solution or the antifreeze mass fraction. This method, since it is based only on the analysis of temperature evolution, is easy to use and allows simple and fast measurements. However, while the results are satisfactory for MPG and MEG, the model could be improved and some simplifications, in particular the assumption of temperature homogeneity in the sample in the first instants of crystallisation, are to be completely justified. Besides, our experimental freezing curve of ethanol is quite far from the data found in the literature and the error analysis does not explain this deviation. New experiments are under way to ameliorate the use of the sensor with ethanol; a detailed crystallisation model for small-volume samples of undercooled water–antifreeze mixtures will soon provide information useful in improving the method.

The tests showed satisfactory reliability and accuracy (still to be improved for ethanol, although the use of our experimental freezing curve ameliorates the results) of the device used for in-line measurements of antifreeze concentration in secondary refrigerant loops. This small sensor covers a wide range of applications, from the control of cold distribution systems to the investigation of thermodynamic equilibrium between solid and liquid phases in ice slurry: indeed, by comparing the temperature of the slurry and the antifreeze concentration in the residual liquid (measured by the sensor), it should be possible to check whether their values are on the freezing curve or not. Due to its simple principles of operation, the cost of this device should be low, the only technical difficulty remains in the need of precise and relatively quick temperature measurements; the data processing being easily done by a personal computer.

## References

[1] O. Lottin, C. Epiard, Dependence of the thermodynamic properties of ice slurries on the characteristics of marketed antifreezes, Internat. J. Refrig. 24 (2001) 455–467.
[2] V. Ayel, O. Lottin, E. Popa, H. Peerhossaini, On-line measurement of the antifreeze mass fraction in aqueous solutions, in: Internat. Congress Refrig., Washington DC, 2003.
[3] O. Bel, A. Lallemand, Etude d'un fluide frigoporteur diphasique. 1 : Caractéristiques thermophysiques intrinsèques d'un coulis de glace, Internat. J. Refrig. 22 (1999) 164–174.
[4] Å. Melinder, Enthalpy-phase diagrams of aqueous solutions for ice-slurry applications, in: Fifth Workshop on Ice Slurries of the IIR, Stockholm, Sweden, 2002, pp. 107–118.
[5] Å. Melinder, Thermophysical Properties of Liquid Secondary Refrigerant, International Institute of Refrigeration, 1997.
[6] Å. Melinder, Accurate thermophysical properties values of water solutions are important for ice slurry modeling and calculations, in: Third Workshop on Ice Slurries of the IIR, Lucerne, Switzerland, 2001, pp. 11–18.
[7] P. Papon, J. Leblond, P.H.E. Meijer, Physique des Transitions de Phase : Concepts et Applications, Dunod, Paris, 1999.
[8] S. Okawa, A. Saito, R. Minami, The solidification phenomenon of the supercooled water containing solid particles, Internat. J. Refrig. 24 (2001) 108–117.
[9] S. Okawa, A. Saito, H. Suto, The experimental study of supercooled water using metallic surface, Internat. J. Refrig. 25 (2002) 514–520.